An eddy-permitting finite-element model for the North Atlantic

Sergey Danilov, Gennady Kivman, and Jens Schröter
Alfred Wegener Institute for Polar and Marine Research
Postfach 12-01-61, 27515 Bremerhaven, Germany

A 3D finite-element primitive-equation ocean model (FEOM) based on tetrahedron partitioning of the computational domain is developed (Danilov et al., 2004). Due to flexibiity in mesh refinement the FEOM provides a tool for modelling the influence of small scale phenomena unresolved by current climate models on large scale ocean circulation.

The model is applied to simulate the North Atlantic thermohaline circulation at eddy-permitting resolution (0.2°–2°). It relies on a horizontally refined mesh in regions of steep topography and allows the sloping bottom to be represented within the z-coordinate vertical discretization, similar to the so called shaved cell approach (Fig. 1). It is the first time this approach is used to model large-scale ocean circulation.

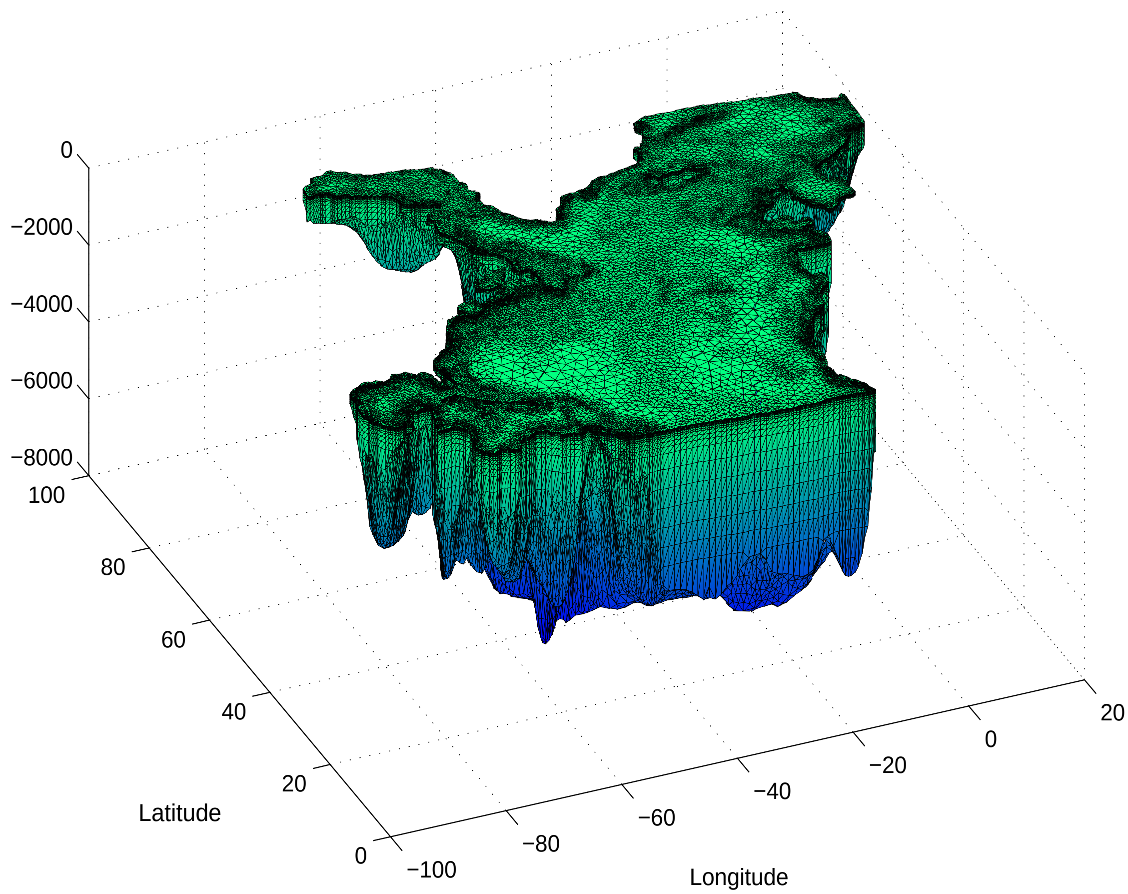

Figure 1: 3D mesh

The FEOM performance in the North Atlantic was compared with that of other models in existence. The meridional overturturning circulation and heat transport are in good agreement with those produced by the DYNAMO project models (Willebrand et al., 2001). The maximum overturning cell is 15.5 Sv and its position is almost identical to that obtained in a $1/10^0$ simulation (Smith et al., 2000). The maximum heat transport is around 1 PW which is in agreement with other models.

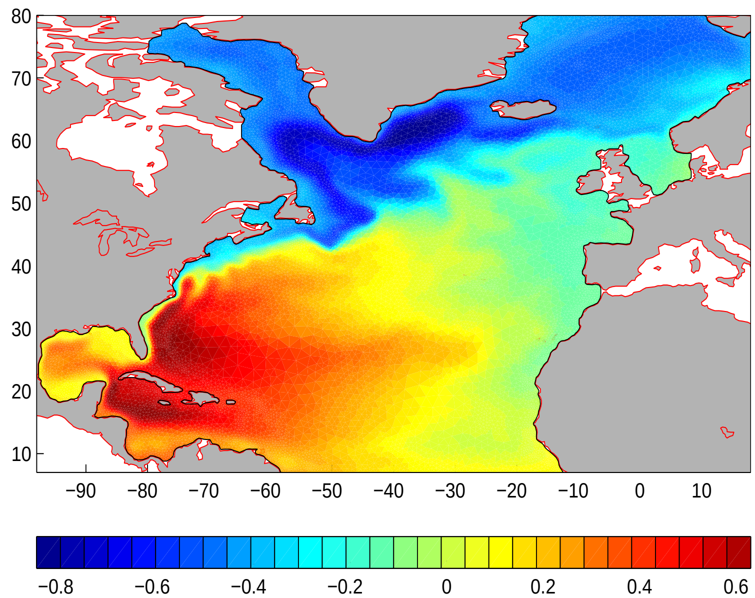

Figure 2: Mean SSH (m).

The mean sea surface height demonstrates the presence of the Gulf Stream recirculation reproduced only by the ISOPYCNIC model of DYNAMO (Fig. 2). When restoring of tracers is applied in the Bay of Cadiz, the model is able to develop the Azores Current of sufficient strength, comparable to that of ISOPYCNIC and maintain the Mediterranean salinity tongue. The annual mean transports of the Gulf Stream and Deep Western Boundary Current at 27°N are of 37 Sv and 17 Sv with core velocities of about 1 m/s and 12 cm/s respectively.

References

[1] Danilov, S., Kivman, G., and Schröter, J. (2004) A finite element ocean model: principles and evaluation. Ocean Modelling 6, 125–150.

[2] Smith, R.D., Maltrud, M. E., Bryan, F.O., and Hecht, M.W. (2000) Numerical simulation of the North Atlantic Ocean at 1/10°. J. Phys. Ocean. 32, 1532–1561.

[3] Willebrand, J., Barnier, B., Böning, C., Dietrich, C., Killworth, P.D., Le Provost, C., Jia, Y., Molines, J.-M., and New, A.L. (2001) Circulation characteristics in three eddy-permitting models of the North Atlantic. Progr. Ocean. 48, 123–161.

Numerical investigation of ocean mixed layer in response to moving cyclone : Sensitivity to model resolution

A.A.Deo, D.W.Ganer and P.S.Salvekar

Indian Institute of Tropical Meteorology, Pune 411 008, India
E-mail : aad@tropmet.ernet.in

Introduction

Present work deals with the sensitivity studies of the upper mixed layer response to an idealized Indian Ocean cyclone using different horizontal resolution of the simple ocean model. In the earlier studies the surface circulation and mixed layer depth (MLD) variation in response to moving cyclones in the Indian Ocean has been studied [1,3,5]. The model used in this study is a simple 1½ layer reduced gravity ocean model over the tropical Indian Ocean (35°E-115°E, 30°S-25°N) with one active layer overlying a deep motionless inactive layer[5]. The initial thermocline is assumed to be 50 m deep and the gravity wave speed is 1m/s. The initial temperature in the mixed and bottom layer are considered as 29°C and 23°C.

Numerical experiments and discussion of results

The horizontal model resolution of the model which is used for control experiment is ½ ° x ½ °. The model cyclone assumes a symmetric rankine vortex having radius 400 km and maximum winds 20 m/s. This vortex is allowed to move along northward track in the Bay of Bengal in four days. The track is from the initial position of (90E,6N) to (90E,14N) . The sensitivity of ocean response to model resolution is examined by increasing the resolution to 1/8 ° x 1/8 ° and 1/12° x 1/12 °. The model temperature change is unrealistically high (about 10°C on 4th day) in the case of high resolution. In order to get the realistic model temperature change the temperature gradient is reduced in further sensitivity experiments. The numerical experiments performed are tabulated below.

Expt. No	Parameters changed for Sensitivity study	Horizontal Resolution	Temperature gradients along mixed layer
1	Horizontal resolution (control experiment)	½ ° x ½ °	6 °C / 50m
2	Horizontal resolution	1/8° x 1/8°	6° C / 50m
3	Horizontal resolution	1/12°x1/12°	6° C / 50m
4	Temperature gradient along mixed layer	1/12°x1/12°	5 °C / 50m
5	Temperature gradient along mixed layer	1/12°x1/12°	4 °C / 50m

Figure 1 (a – f) shows the results for the experiment no. 1 to 3 serially, with the mixed layer depth anomaly in the left panel and the temperature change in the right panel. Solid line drawn is the storm track and the dot represents the position of the storm center. It is seen that the maximum cooling of about 3°C occurs right of the track for day 3, which suggests that the mixed layer on the right of the track is cooled more than the left and there is right bias in the temperature field (Fig 1a). Similarly mixed layer depth anomaly and current field also has right bias (Fig 1b). This is in agreement with the earlier model studies[1,2,4]. The model fields became stronger as the resolution is increased (Exp. 2 & 3). The cooling is increased up to 6°C, in a small region for higher resolution (Fig. 1f). The areal extent of the affected region is reduced for the higher resolution. There is marginal difference in the model fields for the resolution of 1/8 °and 1/12 ° (Fig.1c,d,e & f).

The experiments 4 (Fig 1g &h) and 5 (Fig.1 i & j) resulted into reduction by about 2°C in the overestimated values of temperature change Therefore while using high resolution model, parameterisation of temperature needs to be changed and initial temperature difference across mixed layer should be less, for getting realistic temperature change.

References:

1. Behera S.K, Deo A.A, and Salvekar P.S., 1998: Investigation of mixed layer response to Bay of Bengal cyclone using a simple ocean model. Meteorol. Atmos. Phys.,65, 77-91.
2. Chang S.W. & Anthes R.A., 1978: Numerical simulation of the ocean's nonlinear baroclinic response to translating hurricanes. J. Phys. Oceano., 13, 468-480
3. Deo A.A, Salvekar P.S and Behera S.K,2001: Oceanic response to cyclone moving in different directions over Indian Seas using IRG model. Mausam, 52, 163-174.
4. Price J.F., 1981: Upper ocean response to a hurricane. J. Phys. Oceano., 11,153-175.
5. A.A.Deo, D.W.Ganer and P.S.Salvekar, 2003: Ocean mixed layer response to a Bay of Bengal cyclone: A Case Study, WGNE Report, Research activities in Atmospheric and Oceanic modelling, Report no. 33, April 2003, WMO / TD no. XXXX, pp 8.05-8.06

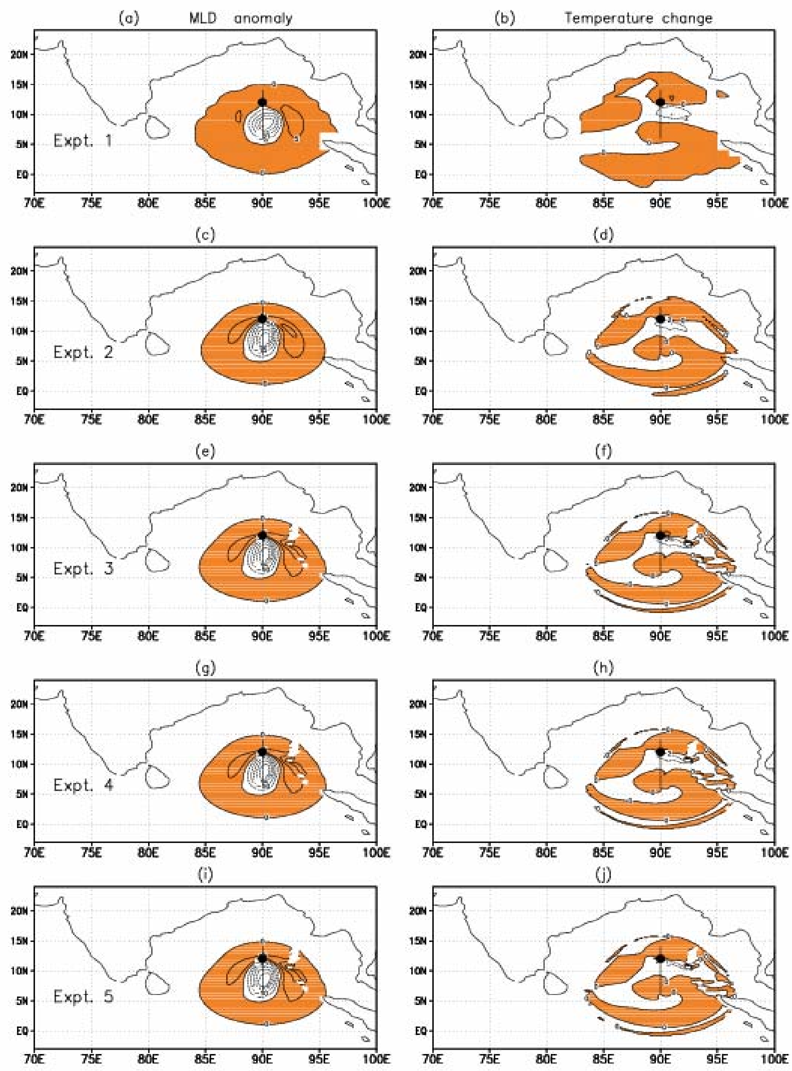

Fig. 1 Mixed layer depth anomalies and temperature change on the third day, for experiments 1-5

Recent and ongoing sea ice modeling activities at UCL-ASTR

T. Fichefet, H. Goosse, V. Dulière, R. Timmermann, and M. Vacoppenolle

Université Catholique de Louvain, Institut d'Astronomie et de Géophysique Georges Lemaître (UCL-ASTR), B-1348 Louvain-la-Neuve, Belgium, E-mail: fichefet@astr.ucl.ac.be.

Recently, a hindcast simulation of the Arctic and Antarctic sea ice variability over the period 1955–2001 has been performed with the UCL-ASTR gobal ice-ocean model [*Fichefet et al.*, 2003a, 2003b]. In this experiment, the model was driven by the National Centers for Environmental Prediction (NCEP) – National Center for Atmospheric Research (NCAR) reanalysis daily surface air temperatures and winds. The other atmospheric input fields consisted of climatologial surface relative humidities, cloud fractions, and precipitation rates. Both the mean state and variability of the ice packs over the satellite observing period are reasonably well reproduced by the model. Over the 47-year period, the simulated ice area in each hemisphere experiences large decadal variability together with a decreasing trend of ~1% per decade. In the Southern Hemisphere, this trend is mostly caused by an abrupt retreat of the ice cover during the second half of the 1970s and the beginning of the 1980s. The modeled ice volume also exhibits pronounced decadal variability, especially in the Northern Hemisphere. Beside these fluctuations, we detected a downward trend in Arctic ice volume of 1.8% per decade and an upward trend in Antarctic ice volume of 1.5% per decade.

The UCL-ASTR sea ice model (LIM) has also been coupled to the French ocean general circulation model OPA. The coupled model was then run on a global domain with a 2 degree mean resolution (ORCA2-LIM configuration). The same forcing as above was used. The model performance has been evaluated with respect to the representation of sea ice and high latitude oceans. The seasonal growth and decay of the sea ice is fairly well simulated in both hemispheres, with ice extent, thickness, and drift in general agreement with observations. The locations of the main sites of deep convection (Labrador and Greenland Seas, and continental shelves of marginal seas of the Southern Ocean) are also well reproduced. Model deficiencies include a slight overstimation of the summer ice extent in the Arctic and a significant underestimation of multiyear ice in the Weddell Sea. Furthermore, the widths of the Arctic Ocean Boundary Current and Antarctic Circumpolar Currents are somewhat overestimated. Sensitivity studies have revealed that the use of a combined forcing dataset is crucial to achieve a reasonable summer sea ice coverage and that the direct utilization of the NCEP–NCAR wind stress data leads to an overestimation of the sea ice velocity. We also showed that a sea surface salinity restoring is necessary to avoid spurious open ocean convection in the Weddell Sea. For further details, see *Timmermann et al.* [2003a, 2003b].

In parallel, we have started to revise LIM in order to remain in the forefront of large-scale sea ice modeling. First, we have replaced the thermodynamic component of the model (which had only three layers) by a multilayer model that explicitly takes into account the effects of sea ice salinity on the specific heat, thermal conductivity, and latent heat of the ice. For this, we basically followed the approach of *Bitz and Lipscomb* [1999]. In addition, we have incoporated in the model the formulation proposed by *Vancoppenolle and Fichefet* [2003] for the spatial and temporal evolution of the sea ice salinity. Given the strong dependence of the ice growth/melt rate on the ice thickness and since the physical properties of sea ice vary widely from one ice type to the other, the inclusion of various ice types and ice thickness categories in LIM is imperative. The relevant ice types that can be present in 100-km-wide oceanic areas (which is the typical size of grid cells of large-scale sea ice models) are : open water, frazil ice, pancake ice, level and ridged first year ice, and level and ridged multiyear ice. We plan to modify LIM so that each grid cell can accomodate these various ice types. Each ice type will be characterized by its own snow and ice thickness distributions and surface and bottom properties (e.g., surface albedo and drag coefficients). Evolution equations for each ice type and thickness category will have to be formulated, and redistribution functions between the different ice types and thickness categories will have to be designed. This work will be done in collaboration with the University of Helsinki, Finland.

Another way of improving the performance of LIM is to assimilate data into the model. This takes adavantage of the great advances that have been made in polar observational capabilities during the last two decades. These advances have led to a rich collection of data on sea ice, including, among others, satellite passive microwave observations of ice motion and concentration. Since it is only very recently that the assimilation of data into large-scale sea ice models has been initated, we propose here to test some of the simplest and low cost data assimilation techniques such as nudging, optimal interpolation, and Kalman filter. In order to reduce as much as possible the computational cost, we plan to evaluate these techniques in a simplified version of LIM using twin experiments (numerical experiments that assimilate model outputs instead of real observations). On the basis of these experiments, we will select the most suitable method and will implement it into the full version of ORCA2-LIM. Previous studies on the assimilation of data into sea ice models showed that problems can arise when assimilating ice motion data alone or ice concentration data alone. Therefore, we project to assimilate both types of data. Two experiments will be then conducted with the coupled model over the last two decades, during which satellite data are available : one with data assimilation and the other without data assimilation. Comparison between results of the two experiments and observations will allow us to evaluate the performance of the data assimilation system.

Acknowledgments. T. Fichefet and H. Goosse are Research Associates at the Belgian National Fund for Scientific Research, and V. Dulière and M. Vancoppenolle are Research Assistants at the Belgian National Fund for Industrial and Agricultural Research. This work is performed within the scope of the Second Multiannual Scientific Support Plan for a Sustainable Development of the Belgian State and the French project of operational oceanography MERCATOR.

References

Bitz, C.M., and W.H. Lipscomb, An energy-conserving thermodynamic model of sea ice, *J. Geophys. Res*., *104*, 15,669-15,677, 1999.

Fichefet, T., H. Goosse, and M.A. Morales Maqueda, A hindcast simulation of Arctic and Antarctic sea ice variability, 1955-2001, *Polar Res*., *22*, 91-98, 2003a.

Fichefet, T., B. Tartinville, and H. Goosse, Antarctic sea ice variability during 1958-1999: A simulation with a global ice-ocean model, *J. Geophys. Res.*, *108 (C3)*, doi: 10.1029/2001JC001148, 2003b.

Timmermann, R., H. Goosse, G. Madec, T. Fichefet, C. Ethé, and V. Dulière, On the representation of high latitude processes in the ORCA-LIM global coupled sea ice–ocean model, *Ocean Modell.*, revised, 2003a.

Timmermann, R., A. Worby, H. Goosse, and T. Fichefet, Utilizing the ASPeCt sea ice thickness dataset to validate a global coupled sea ice–ocean model, *J. Geophys. Res.*, submitted, 2003b.

Vancoppenolle, M., and T. Fichefet, 2004 : An empirical one-dimensional parameterization of the sea ice salinity evolution, In *Proceedings of the ACSYS Final Science Conference (Arctic and Antarctic Research Institute, St. Petersburg, 11–14 November 2003)*, submitted, 2003.

Characteristics of Tropical Indian Ocean during IOD Events

D. W. Ganer, A. A. Deo and P. S. Salvekar
Indian Institute of Tropical Meteorology, Pune-411008, India.
E-mail : tsd@tropmet.ernet.in

Introduction

The inter-annual sea surface temperature (SST) anomalies in the Indian Ocean is of the order 0.5°C which is very less as compared to the other ocean like eastern Pacific ocean. Generally the Indian ocean remains warm with maximum SST of 28°C though the inter-annual variation is weak. The large fluctuations in the equatorial Indian Ocean SST anomalies may play significant role in local climate change. Such events are of great importance and are reported recently as Indian Ocean Dipole (Saji *et al.* 1999; Behera et al. 1999). The present study aims at simulation and understanding of such events using a simple 2½ layer basin scale thermodynamic ocean model.

The Model and Results

In the present work 2½ layer thermodynamic ocean model over the region 35 E-115 E, 30 S - 25 N is used which is fully described in McCreary et al.,1993. The model is spun up for 10 years using daily NCEP climatological winds and heat fluxes obtained from ten years mean for the period 1992 to 2001 to reach the steady state. Further the model integration is carried out using inter-annually varying daily surface winds and heat fluxes from 1992 to 2001. The inter-annual variability in the model SST and currents is very well simulated in the equatorial Indian Ocean. The model simulates large fluctuations with cold SST anomalies in the western equatorial Indian ocean and warm SST anomalies in the eastern equatorial Indian ocean during 1992 (negative IOD) and opposite in the year1994 (positive IOD). Figure 1a & 1b shows that the 1994 event is stronger (temperature difference 3°C) than the 1992 event (temperature difference 2°C). The model current field shows that the equatorial jet is absent in 1994 as also reported by Vinaychandran et. al., 1999, but it is present in 1992 event (Fig. 1c &d) with opposite subsurface currents. The cross equatorial flow is found to be weak during 1994. The analyses of the model currents show that the response of this event is not only confined to the equatorial region but also found in the other parts of tropical Indian ocean. The upwelling coastal Kelvin wave during the positive IOD events influence the circulation in the Bay of Bengal (Fig.1f) in the month of September. This strong propagating Kelvin wave along the perimeter of the Bay sets up southward currents along the eastern boundary of the Bay and reflected Rossby wave sets northward currents along the western boundary of the Bay forming an anti-cyclonic circulation in the Bay. During negative IOD event in 1992, the circulation in the Bay of Bengal (Fig. 1e) is similar to the climatological one and remains unaffected.

The subsurface temperature anomalies during the dipole events 1992 and 1994 are compared. It is seen that the subsurface dipole events during both the years is well simulated by the model. (Figure not shown).

References

- Behera SK, Krishnan R, Yamagata T, 1999. Unusual ocean-atmosphere conditions in the tropical Indian Ocean during 1994. *Geophysical Research Letters* **26:** 3001-3004.
- McCreary J. P., Kundu P. K. & Molinari R. L., 1993. A numerical investigation of dynamics, thermodynamics, and mixed layer processes in the Indian Ocean; *Prog. Ocean*. 31, 181-244
- Vinaychandran P. N., N. H. Saji and T. Yamagata 1999 : Response of equatorial Indian Ocean to an unusual wind event during 1994, Geophys. Res. Lett., 26, 1613-116.
- Saji H., B. N. Goswami, P. N. Vinaychandran and T. Yamagata 1999 : A Dipole mode in the Tropical Indian Ocean, Nature, 401, 360-363

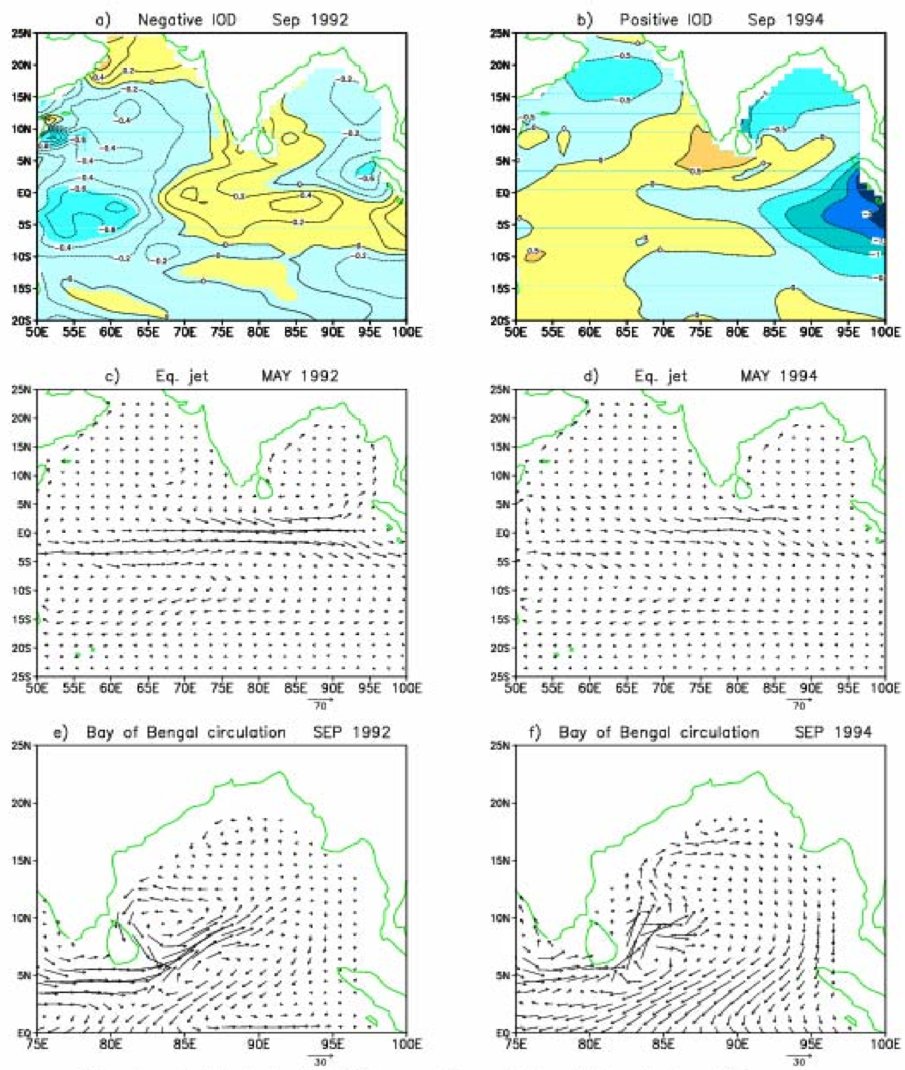

Fig. 1 Model simulated SST anomalies and circulation during IOD events.

Wave simulations for Heligoland.

Lidia Gaslikova,
GKSS Institute for Coastal Research,
Max-Planck-Strasse, D-21502 Geesthacht.
e-mail: lidia.gaslikova@gkss.de

Along with temperature, pressure and precipitation the investigation of 'wave climate' plays an important role in the climate change studies. The extreme wave behavior is of especially great importance due to possible impacts on economics. Understanding trends in occurrences of such events and their future prediction should be considered in the development of coastal areas. In our work we are trying to reconstruct the past and make some projections for the future wave climate in the vicinity of Heligoland Island (German Bight) [2]. The results of the simulations are supposed to be used for analysis of wave extreme events [3]. The most important characteristics that are to be obtained from the simulations are the intensity and frequency of such events (based on the simulated data for the past decades), which can then be exploited in the development and improvement of the coastal protection facilities. Another purpose of such a study is an investigation of the climate change impacts on the coastal wave climate in the North Sea and sensitivity of the wave extremes to different global climate scenarios.

For wave modeling we use the so called K-Model, which is a spectral wave model based on the energy balance equation in terms of energy action density [1]. The model takes into account the time dependent wind field, time varying current-field, variable depth field and time dependent energy flow across the boundaries. It has been adapted for small scale and shallow water applications and tuned for a high performance parallel computer to enable long term forecasting. We are able to treat a domain of 13x16 km around the island (which area is approx. 1 sq. km) with equidistant (100m) spatial resolution and open boundaries for time scales of decades. The boundary conditions have been obtained from the HIPOCAS project [4].

The assessment of model relevance to our problem and sensitivity of the model output to forcing fields has been one of the most important issues.

To check the reliability of the model we have produced a wave hindcast for October 1998 and compared some integrated wave parameters (significant wave height (HS), different periods, etc.) with the measurements from local buoy and radar station. Fig.1 shows wave height curves. It can be seen that for the most part of the considered period observations and model results are in good agreement with each other. The root mean square error between model-buoy is 0.47 and model-radar - 0.72. Wave peak direction (Fig.2) and Tm2 period (not shown) are also reproduced quite good.

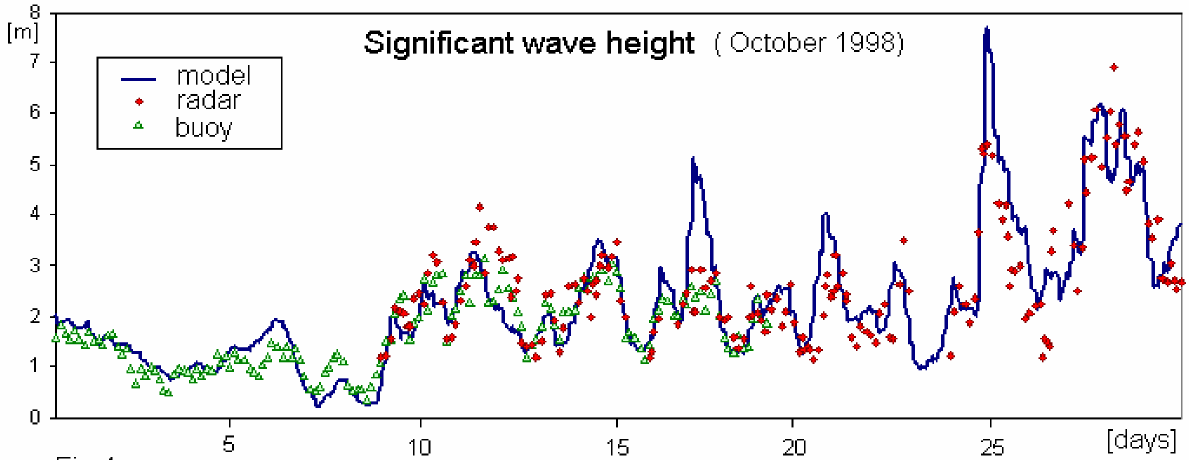

Fig.1

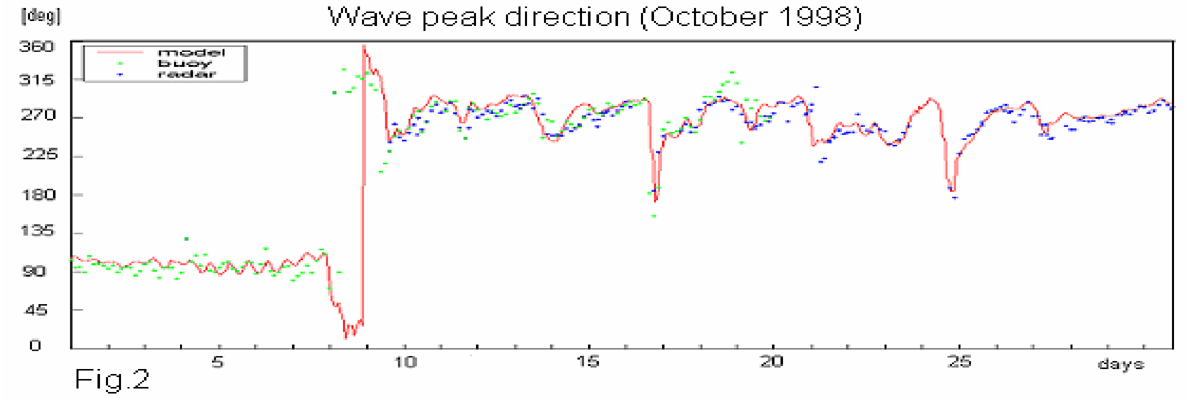

Fig.2

Other tests have been done to estimate the share of influence of different input fields on the integrated wave parameters. This information allows to omit from the model some time consuming but unimportant for our applications processes. So, the model shows that the presence of a current field (the currents in the considered domain are rather stable and driven mainly by tides, their speed does not exceed 1.5 m/s) results in a wave height change of about 10cm near the shore which is about 5 percents of the entire wave height for that moment. Wave periods calculated with currents have strong tidal signal, which is abandoned in the without-current case but after daily smoothing the two cases give almost the same results. So, the current influence in this area is not significant. Simulations with changeable and constant depth have more pronounced difference, within 200 m from the coast line there are about 40 cm higher waves during high tide (wave height is about 3 m). This can be mainly explained by the shoaling effect. This shows the necessity of the variable depth in the model. The last test demonstrates the importance of wind and boundary energy input (Fig.3). Wind component is important because waves are not fully developed on the boundaries and respond to the wind energy within the considered area. Boundary input is more crucial, especially in the case of westerly storms. It seems that waves driven only by local wind couldn't be higher then 2m just because of the small domain area and boundary energy inflow explain more than a half of the wave height. It is especially important to use realistic boundary conditions for our simulations.

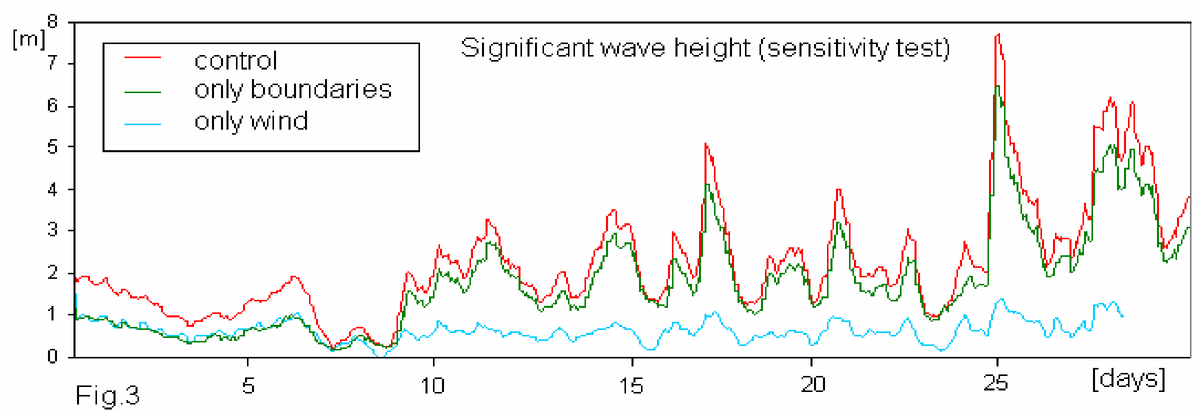

Fig.3

Literature

[1] Schneggenburger, C.,H. Guenther, and W. Rosenthal,1997: Shallow water wave modeling with nonlinear dissipation, *Dt. Hydrogr. Z.*,49, 431-444

[2] Vierfuss, U., 2002: Ermittlung der Seegangsbelastung fuer Helgolaender Molenbauwerke, *HANSA* 139, Heft 1, 68-73

[3] Leadbetter,M.R., Lindgren,G., Rootzen,H., 1983: Extremes and related properties of random sequences and processes, New York: Springer-Verlag

[4] Weisse, R., H. Günther, and F. Feser, 2002: A 40-year high-resolution wind and wave hindcast for the Southern North Sea, *Proceedings, 7th International Workshop on Wave Hindcasting and Forecasting*, Banff, Canada, 2002, 97-104.

The Influence of Coriolis on Instability Wavelengths

Erik Kvaleberg[1], Steven L. Morey and James J. O'Brien
Center for Ocean-Atmospheric Prediction Studies
The Florida State University

The Navy Coastal Ocean Model, a three-dimensional, hydrostatic, primitive equation model developed at the U.S. Naval Research Laboratory (Martin, 2000), is used to study the formation of instabilities on a density front over a shallow, sloping bottom. By applying a uniform and constant surface heat loss to the domain, density increases more rapidly along the coast, and an alongshore thermal wind current develops. Offshore undulations in this current will cause vertical stretching of the water column, and because potential vorticity must be conserved, relative vorticity must compensate by generating cyclonic motions.

The length scale of these instabilities is approximately three times the deformation radius, indicating that the current is baroclinically unstable (Gawarkiewicz & Chapman, 1995). The deformation radius is defined as $R_D = \frac{Nh}{f}$, where N is the buoyancy frequency, h is the local depth and f is the Coriolis parameter. As part of this project, we wish to study the influence of latitude on the instability wavelength by varying the Coriolis parameter. Three experiments are performed, at 60°N, 30°N and at the equator. The surface heat loss is set to 60 Wm^{-2} in all runs, and the topography (Figure 1) depicts an idealized shelf. The planetary beta effect is neglected, because the topographic beta (owing to the sloping bottom) is two orders of magnitude larger.

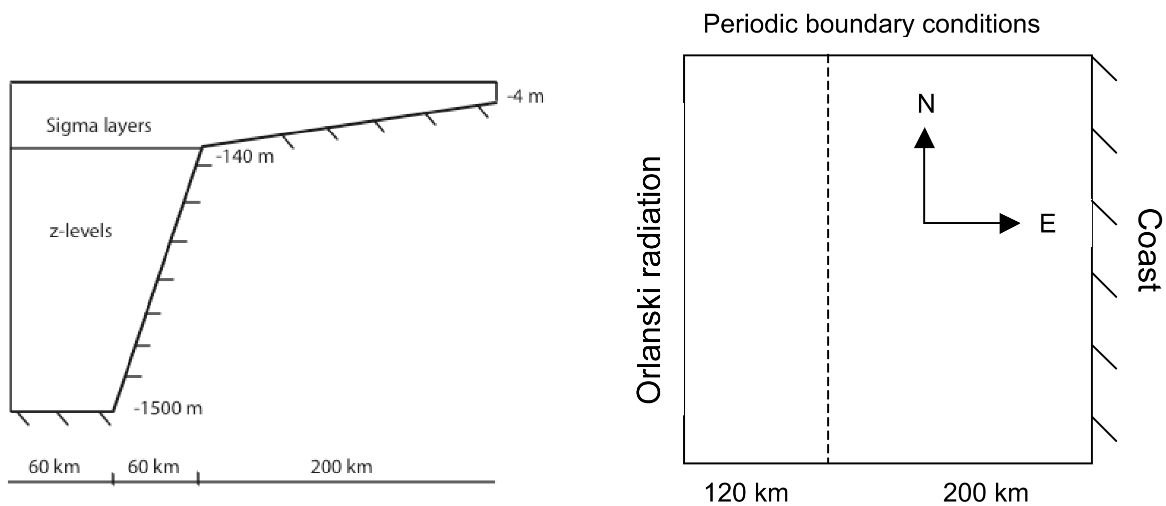

Figure 1. Topography (left) and domain (right) used in the numerical experiments.

[1] erik@coaps.fsu.edu

From the expression for the deformation radius, it is expected that the instability length scale decreases with increasing latitude. At the equator then, the scale should tend to infinity and no instabilities be present. Presented below (Figure 2) are sea surface density fields after 60 days of cooling for each latitude. Clearly, latitude plays an important role in determining the instability scale, but it also seems to affect the amount of cross shelf mixing, which is important for biology and chemistry.

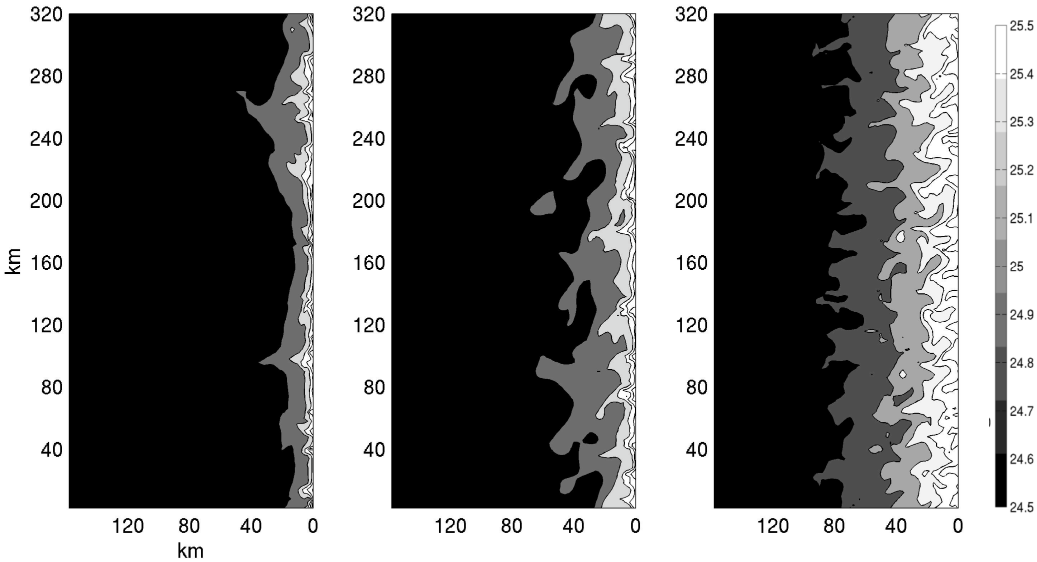

Figure 2. Sea surface density (in $kg\,m^{-3} - 1000$) after 60 days of cooling at the equator (left), 30°N (middle) and 60°N (right).

It is probably difficult to observe this in nature as clearly as it is shown here, since the presence of wind and variable topography will modify the instabilities, however satellite images of sea surface temperature may prove useful in this respect.

Acknowledgments: This research was funded by the Office of Naval Research through a Secretary of the Navy grant awarded to Dr. James J. O’Brien, and by a NASA Office of Earth Science grant.

References:

- Gawarkiewicz, G. and D. C. Chapman, A numerical study of dense water formation and transport on a shallow, sloping continental shelf, J. Geophys. Res., 100, C3, 4489-4507, 1995.

- Martin, P.J., A description of the Navy Coastal Ocean Model Version 1.0, NRL Report: NRL/FR/7322-009962, Naval Research Laboratory, Stennis Space Center, MS, 39 pp. 2000.

Response of a two-layer estuary to freshwater inflow and wind: a case study of the Baltic Sea

H.E.M. Meier[1] and F. Kauker[2]

The Baltic Sea is one of the world's largest brackish-water sea areas, with large horizontal and vertical salinity gradients. The average salinity amounts to about 7.4 $^o/_{oo}$ (Meier and Kauker, 2003a). A large net freshwater supply mainly from river discharge of about 15,000 to 16,000 $\mathrm{m^3\,s^{-1}}$ in combination with the hampered water exchange through the Danish Straits causes this low salinity. Decadal salinity variations are of the order of 1 $^o/_{oo}$, and no long-term trend is detectable during 1902-1998 (Fig. 1).

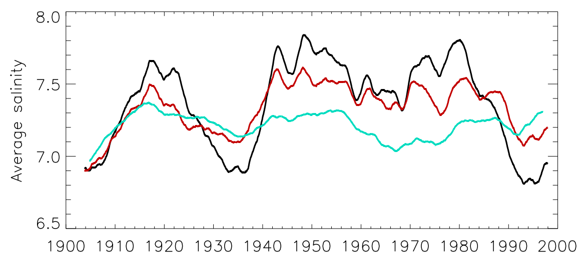

Figure 1: *2-year running mean simulated salinity in the Baltic Sea (in $^o/_{oo}$): reference run (black), sensitivity experiment with climatological monthly mean freshwater inflow (red), and sensitivity experiment with climatological monthly mean freshwater inflow and 4-year high-pass-filtered sea level pressure and associated surface winds (blue).*

Hindcast simulations for the period 1902-1998 have been performed using the 3-D coupled ice-ocean model RCO for the Baltic Sea (Meier and Faxén, 2002; Meier et al., 2003). Daily sea level observations at the open boundary in Kattegat, monthly basin-wide discharge data, and reconstructed atmospheric surface data have been used to force RCO. The reconstruction utilizes a statistical model to calculate daily sea level pressure and monthly surface air temperature, dew-point temperature, precipitation, and cloud cover fields (Kauker and Meier, 2003). Sensitivity experiments have been performed to explore the impact of the natural fresh- and saltwater inflow variability on the salinity of the Baltic Sea (Meier and Kauker, 2003a). The decadal variability of the average salinity is explained partly by decadal volume variations of the accumulated freshwater inflow from river runoff and net precipitation and partly by decadal variations of the large-scale sea level pressure over Scandinavia (Fig. 1). During the last century two exceptionally long stagnation periods are found, the 1920s to 1930s and the 1980s to 1990s. During these periods precipitation, runoff and westerly winds were stronger and salt transports into the Baltic were smaller than normal. As the response time scale on freshwater forcing of the Baltic Sea is about 35 years, seasonal and year-to-year changes of the freshwater inflow are too short to affect the average salinity significantly. We found that the impact of river regulation which changes the discharge seasonality is negligible.

As recent results of some regional climate models suggested a significant increase of precipitation in the Baltic catchment area due to anthropogenic climate change, the response of salinity in

[1]Swedish Meteorological and Hydrological Institute, Rossby Centre, SE-60176 Norrköping, Sweden, e-mail: markus.meier@smhi.se

[2]Alfred Wegener Institute for Polar and Marine Research, Bussestr. 24, PoBox 120161, D-27515 Bremerhaven, Germany, e-mail: fkauker@awi-bremerhaven.de

the Baltic Sea to changing freshwater inflow is investigated. Therefore, model simulations with modified river runoff and precipitation for the period 1902-1998 have been performed (Meier and Kauker, 2003b). Thereby, it is assumed that the Kattegat deepwater salinity of about 33 $^o/_{oo}$ will not change regardless of the changed freshwater supply. We found that even for a freshwater supply increased by 100% compared to the period 1902-1998 the Baltic Sea cannot be classified as a freshwater sea. A still pronounced halocline separates the upper and lower layer in the Baltic proper limiting the impact of direct wind mixing to the surface layer. A calculated phase diagram suggests that the relationship between freshwater supply and average salinity of the final steady-state is non-linear (Fig. 2). The results of RCO are in agreement with an analytical

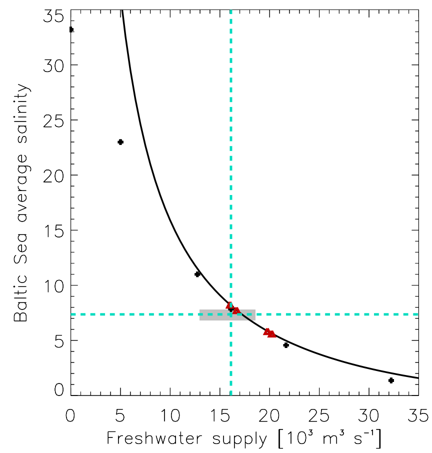

Figure 2: *Steady-state Baltic Sea average salinity as a function of the freshwater supply. The solid line shows analytical results of a steady-state Baltic Sea model. The plus signs denote steady-state RCO results for the period 1969-1998. The red triangles show scenario results based upon changes of freshwater inflow in regional climate models. In addition, the present climate (1902-1998) with a mean salinity of* $7.4\,^o/_{oo}$ *and a mean freshwater inflow of* $16,000\,m^3\,s^{-1}$ *is shown (blue dashed lines). Minimum and maximum values of the 4-year running means indicate the natural variability (shaded area).*

steady-state model which is supposed to work for freshwater changes smaller than 30 % (Meier and Kauker, 2003b). The latter model is applied in 4 scenarios for the average salinity of the Baltic Sea (Fig. 2). The largest increase of the freshwater inflow of 16 % is found in a B2 scenario utilizing data from ECHAM4/OPYC3 of the Max-Planck-Institute for Meteorology in Hamburg, Germany. The corresponding estimated average salinity is about 35 % lower than the present value. Such a large change is outside the range of natural variability of the past century.

References

Kauker, F., and H.E.M. Meier, 2003: Modeling decadal variability of the Baltic Sea: 1. Reconstructing atmospheric surface data for the period 1902-1998. *J. Geophys. Res.*, 108(C8), 3267.

Meier, H.E.M., and T. Faxén, 2002: Performance analysis of a multiprocessor coupled ice-ocean model for the Baltic Sea. *J. Atmos. Oceanic Technol.*, 19, 114-124.

Meier, H.E.M., and F. Kauker, 2003a: Modeling decadal variability of the Baltic Sea: 2. Role of freshwater inflow and large-scale atmospheric circulation for salinity. *J. Geophys. Res.*, 108(C11), 3368.

Meier, H.E.M., and F. Kauker, 2003b: Sensitivity of the Baltic Sea salinity to the freshwater supply. *Clim. Res.*, 24, 231-242.

Meier, H.E.M., R. Döscher, and T. Faxén, 2003: A multiprocessor coupled ice-ocean model for the Baltic Sea: Application to salt inflow. *J. Geophys. Res.*, 108(C8), 3273.

Observed and Simulated Variability of Ocean Currents on Seasonal and Intra-Monthly Scales

Yurii D. Resnyansky and Alexander A. Zelenko

Hydrometeorological Research Center of the Russian Federation,
Bol. Predtechesky per., 11-13, 123242 Moscow, Russia *E-mail: resn@mecom.ru*

A set of numerical experiments has been conducted using an ocean general circulation model (OGCM) developed in Hydrometcenter of Russia (*Resnyansky and Zelenko, 1999*). They are aimed at studying the dependence of dynamical characteristics simulated by the model (kinetic energy, vertical structure and temporal variability of ocean currents) on horizontal diffusivity A_H in the equations of heat and salt transport. Finding the dependence of this sort is vital for estimating the relative role of different processes in generating the mean structure and temporal variability of dynamic and hydrographic fields, as well as for tuning the model in order to attain the most possible agreement with observations. In the course of experiments the ability of OGCM to reproduce the structure of temporal variability on seasonal and intra-monthly time scales was also estimated through the comparison with direct current meter records.

To estimate the sensitivity of model results to variations of thermodynamic parameters, three other than that identical model runs have been performed differing only in horizontal diffusivity A_H = 10^3, 10^4 and 10^5 m^2 s^{-1}. In each of the runs the evolution of oceanic fields forced by realistic atmospheric forcing over 24 years was simulated starting from rest with climatological temperature and salinity distributions. The forcing (surface wind stress and heat/fresh water fluxes) was specified using 6-hourly data of NCEP-DEO AMIP-II Reanalysis (*Kanamitsu et al., 2002*) over 1979–2002 in combination with relaxation of the computed near-surface water temperature and salinity values to specified distributions from the WOA-98 atlas assuming relaxation coefficient $c_r^{-1} = 30\ d$. The model integrations were performed in a global domain (excluding the Arctic basin to the north of 77.5° N) on 2°×2° (2°×1° in near equatorial band) grid with 32 level in the vertical.

As an example, a comparison of computed current speeds with current meter records appears in Fig. 1. Here, time series of current speed in the Northwest Pacific over the period from July 1980 to May 1981 are depicted for three depths: in the upper layer ($z = 500$ m), in the main thermocline ($z = 1200$m) and in deep layer ($z = 4000$ m). As is seen, according to the measurements, the currents strength (mean speed level $\overline{U}$) keeps almost invariant, about 10 cm s^{-1} over a rather broad range of depths. In the model, the mean speed level appears to be underestimated by several times due to, obviously, comparatively course horizontal resolution.

Nonetheless, in the upper layer ($z = 500$ m) the simulations reproduce rather realistically not only general features of the temporal variability on seasonal and intra monthly time scales, but also the most remarkable episodes of the currents temporal changes: almost two-fold intensification in November–December, 1980 and in March–April, 1981; variations with prevailing periods of about two weeks in between these episodes; decreasing intensity to the end of the period considered.

Mutual similarity of observed and computed individual peculiarities weakens with increasing depth ($z = 1200$ m and $z = 4000$ m), though some common features of observed variability remains in model simulations as well. Besides, the impact of A_H variations on the model results, distinctly seen in the upper layer ($z = 500$ m), slackens at these depths. As A_H increases, the mean speed level decreases: from $\overline{U}$ ~ 5 cm s^{-1} with A_H = 10^3 m^2 s^{-1} down to $\overline{U}$ ~ 2 cm s^{-1} with A_H = 10^4 m^2 s^{-1} and $\overline{U}$ ~ 1.5 cm s^{-1} with A_H = 10^3 m^2 s^{-1}. Thus, in the upper part of the A_H variations range considered here the tendency appears for "satiation" of the model response to variations of the parameter. These peculiarities may be evidently explained by enhanced smoothing of the lateral water density gradients in the baroclinic layer with increasing A_H .

Similar "satiety" may be also noticed in integral dynamic characteristics, such as kinetic energy *KEN* averaged over the World Ocean. Mean levels of *KEN* for A_H =10^3, 10^4 и 10^5 m^2 s^{-1} are 0.25, 0.16 and 0.14 J m^{-3} correspondingly.

Reduction of the similarity with increasing depth may be considered as evidence that in the upper layers the currents variability is determined to a greater degree by the direct response of the ocean to atmospheric forcing (it is specified by "realistic" data in the experiments considered), and with increasing depth the role of internal ocean dynamics rises.

Acknowledgment: This work was supported by the Russian Foundation for Basic Research grant No. 03-05-64814.

References

Data from Deep Water Current Meter Moorings, 1973–2000. CD-ROM, Publ. by OSU Buoy Group, Oregon State University, 2002.

Kanamitsu, M., W. Ebisuzaki, J. Woollen, S-K Yang, J.J. Hnilo, M. Fiorino, and G. L. Potter. NCEP-DEO AMIP-II Reanalysis (R-2). *Bul. Amer. Met. Soc.*, 2002, **83**, 1631-1643.

Resnyansky, Yu.D. and A.A. Zelenko, 1999: Effects of synoptic variations of atmospheric forcing in an ocean general circulation model: Direct and indirect manifestations. *Russian Meteorology and Hydrology*, No. 9, 42-50.

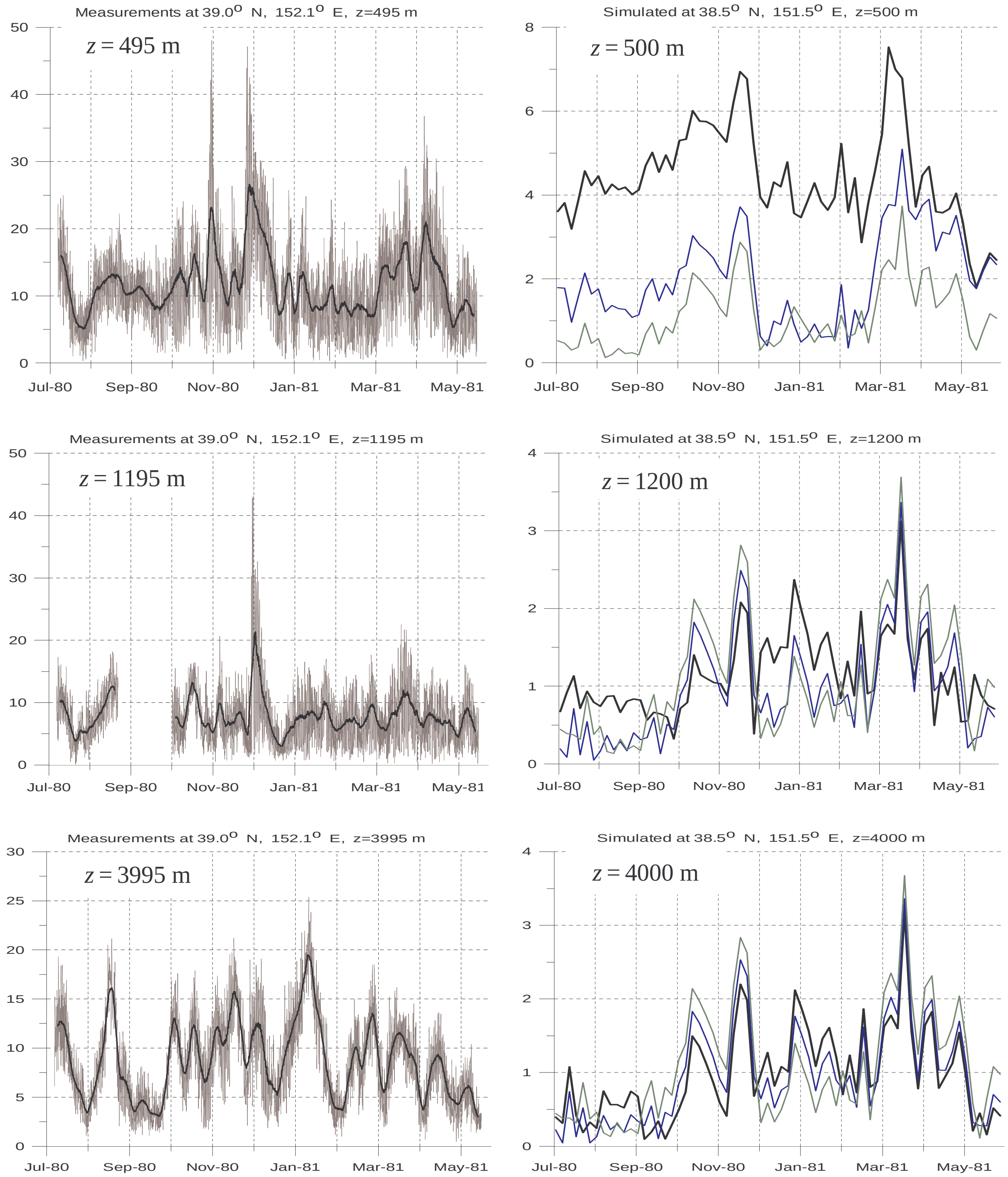

Fig. 1. Measured and simulated July 1980–May 1981 time series of current speed (cm s^{-1}) in the Northwestern Pacific at three different depths: in the upper layer, in the main thermocline and in deep ocean.

Left column – current meter measurements during WESTPAC 1 Experiment (39.0° N, 152.1 E) (*Data from Deep Water Current Meter Moorings, 2002*.). Gray thin line – hourly data, black thick line – 5 days running average.

Right column – OGCM simulations on 2°×2° grid with 6-hourly atmospheric forcing from NCEP-DEO Reanalysis-2 (*Kanamitsu et al., 2002*). Curves in black, in blue, and in green (drawn through data points at 5 days intervals) relate to model runs with horizontal diffusivity $A_H = 10^3$, 10^4 and 10^5 $m^2 s^{-1}$ correspondingly.

Thermodynamics of the oceanic general circulation

Shinya Shimokawa * and Hisashi Ozawa **
* National Research Institute for Earth Science and Disaster Prevention, Tsukuba 305-0006, Japan
(simokawa@bosai.go.jp)
** Frontier Research System for Global Change, Yokohama 236-0001, Japan

1. Introduction

It is well known that thermohaline circulation has multiple steady states under the same set of boundary conditions (Stommel, 1961). However, the mechanism of the transitions among the multiple steady states is not yet fully understood. It is also known that a nonlinear system will evolve along a path favoring the maximum entropy production among manifold possible paths (the principle of maximum entropy production, Sawada, 1981). However, there is no study that tests the principle for the ocean system. The objectives of this study are to develop a method evaluating the rate of entropy production in large-scale circulation models and to examine the principle for the ocean system by applying to the method to an oceanic general circulation model.

2. Calculation method of entropy production

The rate of entropy production is calculated in large-scale circulation systems such as

$$dS/dt = \int \rho c/T\ \partial T/\partial t\ dV + \int F_h/T\ dA - \alpha k \int \partial C/\partial t\ \ln C\ dV - \alpha k \int F_s \ln C\ dA \qquad (1)$$

where ρ is the density, c is the specific heat at constant volume, T is the temperature, $\alpha=2$ is van't Hoff's factor representing the dissociation effect of salt into separate ions (Na^+ and Cl^-), k is the Boltzmann constant, C is the number concentration of salt per unit volume of sea water, F_h and F_s are the heat and salt fluxes per unit surface area, defined as positive outward, respectively. The first term on the right hand side represents the rate of entropy increase in the ocean system due to heat transport, and the second term represents that in the surrounding system. The third term represents the rate of entropy increase in the ocean system due to salt transport, and the fourth term represents that in the surrounding system. Overall, Equation (1) represents the rate of entropy increase of the whole system. This equation is applicable to a large-scale circulation model whose scale of resolution is coarser than the dissipation scale because it dose not include a microscopic representation of the dissipation process (Shimokawa and Ozawa, 2001).

3. Model description and Experimental method

The numerical model used in this study is the GFDL MOM version 2. The model domain is a rectangular basin with a cyclic path, representing an idealized Atlantic Ocean. The horizontal grid spacing is 4 degrees. The depth of the ocean is 4500 m with twelve vertical levels. Our experiments consist of three phases: (1) spin-up under restoring boundary conditions for 5000 years, (2) integration under mixed boundary conditions with a high-latitude salinity perturbation for 500 years, and (3) integration under mixed boundary conditions without perturbation for 1000 years. As a result of phase (1), the system reaches a statistically steady state with northern sinking circulation (N_{RBC}, Fig. 1a). In phase (2), the system moves to a state which is determined by the perturbation applied. In phase (3), the system is adjusted satisfactorily to the boundary condition without perturbation. Then, in some cases, the system returns to the initial state, while in other cases, it does not, instead remaining in the state of being determined by the perturbation or moving to a different steady state which is independent of the perturbation. If a new steady state is obtained, procedures (2) and (3) are repeated using the new steady state as the initial state. If a new steady state is not obtained, these procedures are repeated using a different salinity perturbation. As a result, a series of multiple steady states under the same set of wind forcing and mixed boundary conditions are obtained (Fig. 1). The standard salinity perturbation used in this study (Δ in Fig. 2) is 2×10^{-7} kg m^{-2} s^{-1}, which is applied to the north of 46N or the south of 46S.

4. Results of the spin-up experiment

The oceanic circulation becomes statistically steady after the year 4000 and its flow pattern shows a basic one in the idealized Atlantic Ocean (N_{RBC}, Fig. 1a). In the steady-state after the year 4000, for both heat and salt transports, the entropy increase rates for the ocean system are zero whereas those for the surrounding system show positive values. The zero increase rates represent the fact that the ocean system is in a steady-state. Heat and salt are transported from equatorial (hot and salty) to polar (cold and less salty) regions by the steady-state circulation. These irreversible transports contribute to the entropy increase in the surrounding system. In this sense, the surrounding system is not in a steady state, even though the ocean system is in a steady-state.

5. Results of the transition experiments

The results of the transition experiments are summarized in Fig. 2. Starting from S1 (Fig. 1e), the system moves to S2 (Fig. 1f) regardless of the sign of the perturbation (r04 and r05); whereas starting from S2, the system does not return to S1, but remains in the initial state (S2) regardless of the sign of the perturbation (r08 and r09). Likewise, the system moves from S3 to S4 (r14 and r15), whereas it does not return to the initial state (r18 and r19). When these transitions occur (r04, r05, r14 and r15), the rates of entropy production in the final states are always higher than those in the initial states (see Fig. 2). These results show that the transition from a state with lower entropy production to a state with higher entropy production tends to occur, but the transition in the inverse direction does not occur, i.e. the transition is *irreversible* or *directional* in the direction of the increase of the rate of entropy production. On the other hand, transitions in mutual directions between southern sinking and northern sinking are possible depending on the direction of the perturbation (r06, r12, r16 and r13). These results may appear to contradict the principle of maximum entropy production. However, we can show that the decrease is only caused by the negative perturbation applied to the sinking region which destroys the initial circulation altogether (Shimokawa and Ozawa, 2002). After the destruction, the entropy production is found to increase as a new circulation develops. All these results tend to support the hypothesis that a nonlinear system, when perturbed, is likely to move to a state with maximum entropy production.

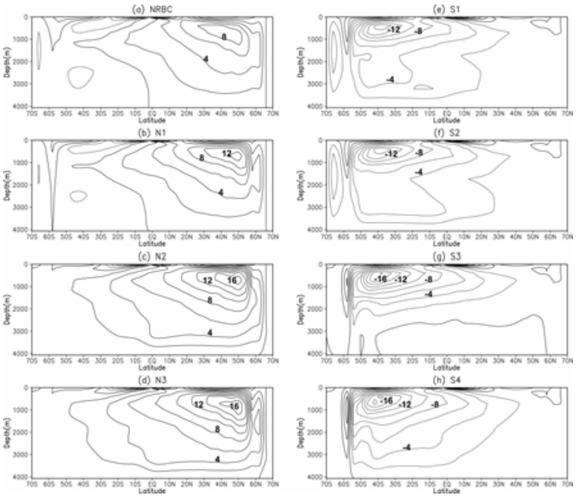

Fig. 1 All steady states obtained from this study. (a) N_{RBC}, (b) N1, (c) N2, (d) N3 (e) S1, (f) S2, (g) S3, (h) S4. Fields shown are zonally integrated meridional stream function at year 5000 for (a) spin-up and at year 1500 for (b) r06, (c) r02, (d) r16, (e) r01, (f) r04, (g) r13 and (h) r14. The contour line interval is 2 SV (10^6 m^3 s^{-1}). The capital letters "N" and "S" refer to northern sinking and southern sinking, respectively. N_{RBC} is a unique solution under restoring boundary conditions.

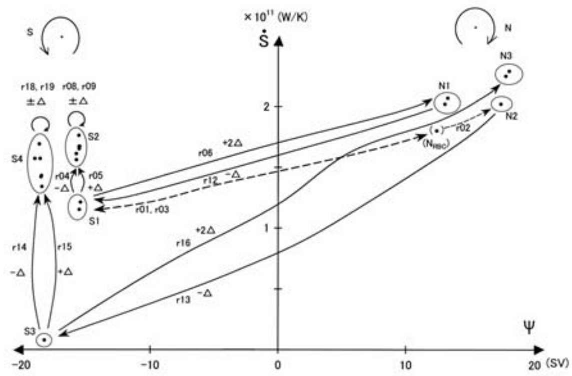

Fig. 2 The relationship between transitions among multiple steady states and rates of entropy production. The vertical axis (S) indicates the rate of entropy production, and the horizontal axis (Ψ) shows the maximum value of the zonally integrated meridional stream function for the main circulation. The dots are corresponding to the steady states (initial and final states) of each experiment. The circles surrounding the dots show the circulation pattern (e.g. N1). The arrows show the direction of the transitions. The symbols besides the arrows show the experiment number and the perturbation used in the experiment (e.g. r04 and -Δ).

REFFERENCES: Sawada, Y. (1981) Prog. Theor. Phys., **66**, 68-76., Stommel, H. (1961) Tellus, **13**, 224-230., Shimokawa, S. and H. Ozawa (2001) Tellus, **A53**, 266-277., Shimokawa, S. and H. Ozawa (2002) Q. J. Roy. Meteorol. Soc., **128**, 2115-2128.

Ocean Data Assimilation at ECMWF

Arthur VIDARD David ANDERSON Magdalena BALMASEDA Tim STOCKDALE Alberto TROCCOLI
European Centre for Medium-range Weather Forecast
Shinfield Park Reading Berkshire RG2 9AX, UK

section 3: in collaboration with
Keith HAINES Xiaobing ZHOU Ivan ASTIN
Environmental Systems Science Centre
Reading University
Reading RG6 6AL, UK

1 In situ temperature observing system experiment

The relative merits of the TAO/TRITON and PIRATA mooring networks, the VOS XBT network, and the ARGO float network are evaluated through their impact on ocean analyses and seasonal forecast skill. An ocean analysis is performed in which all available data are assimilated. In two additional experiments the moorings and the VOS data sets are withheld from the assimilation. To estimate the impact on seasonal forecast skill, the set of ocean analyses is then used to initialise a corresponding set of coupled ocean-atmosphere model forecasts. A further set of experiments is conducted to assess the impact of the more recent ARGO array. The forecasts mainly indicate that, in the tropical pacific, the TAO in-situ temperature observations are essential to obtain optimum forecast skill. They are best combined with XBT, however, as the combination with XBT data results in better predictions for the east pacific area (Fig. 1 left panel).

2 Altimetry data assimilation in ECMWF seasonal forecast system

In the current ECMWF seasonal forecast system the ocean is initialised by the mean of an Optimal Interpolation scheme using in situ temperature. Three ways of assimilating altimetry data into ECMWF System have been explored. In both the sea level anomaly is translated into a vertical displacement of the Temperature and Salinity profile following Cooper and Haines, 1999 (CH99). This sea-level-derived profiles are then either use as background fields for the OI or used as pseudo-observation and then fed into the temperature OI. The third way is to perform the OI analysis and then apply the CH99 scheme tho this analysis.

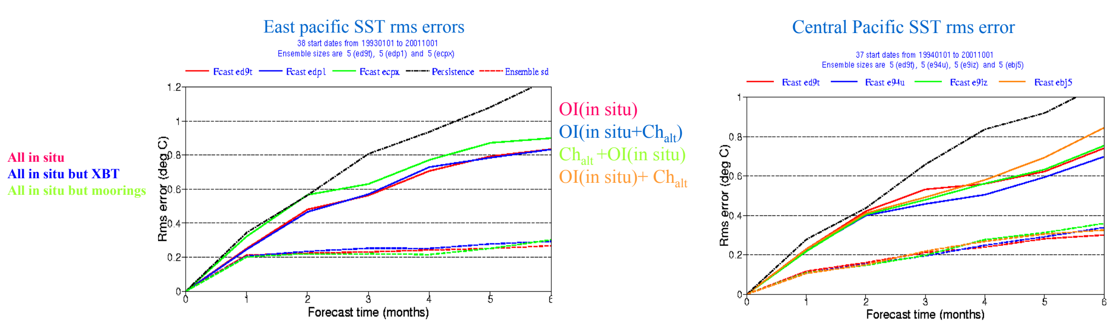

Figure 1: SSTA forecast skill measured by rms-error for coupled experiments. The dot-dash curve is a measure of skill for persistence.

Although both these methods are somewhat more skillful than the temperature only assimilation (see for instance Fig. 1 right panel), since to compute sea level anomaly, we use the mean sea level from a previous model run, the analysis is far to biased toward this run. Ongoing plans are to use other mean seal levels, such as CLS mean dynamic topography or products derived from the GRACE geoid mission.

3 Assimilation of salinity data

Assimilating salinity data, along with temperature, into ocean models should allow for the better analysis of water properties and volumes over whole regions of the ocean. This would allow for better assessment of climatically important changes in water characteristics, that are normally only possible from repeat section hydrography.

A two-stage process is used. (1) Temperature (from Argo and other data sources, XBT, TAO ...) is assimilated and the salinity is incremented to retain the S(T) relationship present in the model. This has previously been shown to greatly improve the salinity reproduction in the ECMWF model compared with leaving the salinity field unchanged. (2) Then the S(T) (from Argo) is assimilated directly, using a covariance function which is dependent on both horizontal separation and separation in temperature space. The method allows for larger spatial scales to be used, thus allowing a wider influence of the salinity data as a measurement of S(T). Some illustrations of this scale difference from using a conventional covariance function for S will be shown.

Ongoing plans are to produce a 40 year reanalysis of ocean properties and circulation, from which changes in S(T) properties and volumes of water masses can be diagnosed, where and when sufficient data are available.

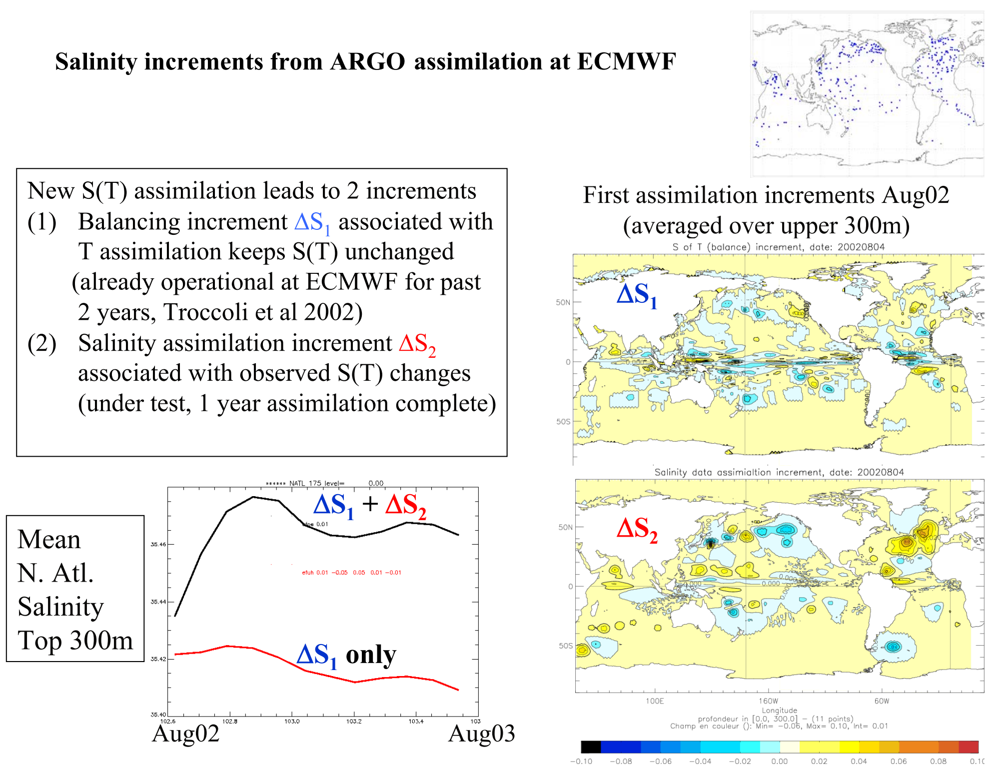

Development of a reduced space adjoint data assimilation technique for numerical simulation of oceanic circulation

Peng Yu[1], Steven L. Morey, and James J. O'Brien
Center for Ocean-Atmospheric Prediction Studies, the Florida State University

Numerical simulation has become one of the most important tools in studying geophysical problems, such as those encountered in physical oceanography and meteorology. The launch of many scientific satellites over recent years has provided scientists access to enormous volumes of data, presenting new opportunities for finding innovative ways to use them. The assimilation of these data into numerical simulations has become a topic of much interest in geophysics. The main objective of this study is to develop and apply a new technique for efficiently using the adjoint method to assimilate satellite altimeter data into a modern fully three-dimensional ocean general circulation model.

There are a number of different methods for data assimilation, classified as function fitting methods, statistical interpolation methods, nudging data assimilation, variational (adjoint) methods and the Kalman filter. An extensive review of these methods can be found in Ghil and Malanotte-Rizzoli (1991) and Le Dimet and Navon (1988). Being one of the best, but also computationally demanding, the adjoint method minimizes the distance between a model solution and the observations, which is called the cost function. This can be defined so that the solution does not have to obey the dynamics of the model exactly by adding a term that measures the model error as in the representer method. The minimization of the cost function gives rise to the weak constraint minimization problem. When the solution is required to satisfy the model exactly, it is referred to as strong constraint minimization. This is done by adjusting the state of the control variables of the model (e.g. initial conditions). An iterative technique is used in which the ocean model is integrated forward in time, followed by a backward integration of an adjoint of the system forced by the observations. By writing the cost function in the form of an inner product, the result of the backward integration of the adjoint model to the initial time will be the gradient of the cost function with respect to the control variables. Thus, an optimization method can be applied to reduce the cost function by changing the control variables at each iteration.

In this study, the adjoint method will be applied to the Navy Coastal Ocean Model (NCOM) in the Gulf of Mexico (Fig. 1). The NCOM is a three dimensional, hydrostatic, primitive equation ocean model with a hybrid sigma (terrain following)/ z-level vertical coordinate recently developed at the U.S. Naval Research Laboratory. The model domain includes the whole Gulf of Mexico and the western Caribbean Sea, from 98.15ºW to 80.60ºW and from 15.55ºN to 31.50ºN, with model equations discretized on a 1/20-degree grid, in latitude and longitude (Morey *et al*., 2003). The model uses 20 sigma layers uniformly distributed in the upper 100 meters and 40 unevenly distributed z-level layers below 100m. Sea surface height data from the Topex/Poseidon satellite altimeter will be assimilated into the model. The computational cost for a complicated model like the NCOM is very expensive, and the adjoint of this model would be even more resource intensive. In order for the technique to be practical for operational use, it is crucial to find a way to reduce the computational cost. For a wide class of oceanographic phenomena, the vertical dimension of the ocean structure can be very well approximated by a single active depth-averaged layer over an infinitely deep layer at rest. This formulation is often called a reduced gravity model, and is much less computationally expensive. For this reason, a backward model based on a reduced gravity formulation will be used as the adjoint, instead of integrating the adjoint of the NCOM directly. This novel approach, termed a "reduced space adjoint technique", will be developed and tested for the first time in a high-resolution model of the Gulf of Mexico. After the forward integration of the NCOM at each time, the first baroclinic mode will be extracted using vertical normal mode decomposition. Since the vertical normal mode decomposition has to be conducted on a non-flat bottom, conventional methods will not be used here. However, two options are taken into consideration: the first one is to compute the vertical modes at each point in the x-y space; the second is to compute the normal modes in a region that is relatively flat compared to the other areas. Cyclostationary Empirical Orthogonal Analysis (Kim, 1997) will then be applied to the output of the model, and the regression method will be used to obtain the first baroclinic mode. Then the adjoint of the corresponding reduced

[1] peng@coaps.fsu.edu

gravity model will be run. The validity and efficiency of this technique will be examined with idealized cases and realistic simulations of the Gulf of Mexico ocean circulation.

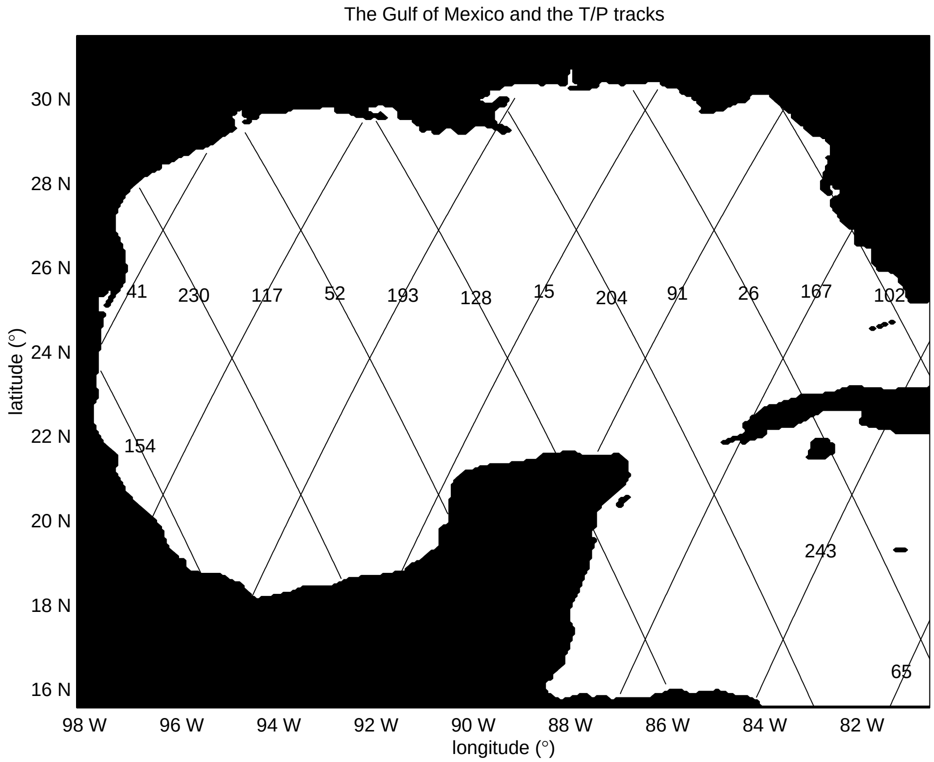

Figure 1. The model domain of the Gulf of Mexico numerical simulation using the Navy Coastal Ocean Model (NCOM). The black lines are Topex/Poseidon tracks.

It is anticipated that this new variation of the adjoint data assimilation technique will dramatically improve the convergence speed and reduce the computational cost so that the technique may be more practically applied to operational oceanography and research in ocean numerical simulation.

Acknowledgements

This work is supported by TOPEX/Poseidon and JASON-1 altimetry project at the NASA JPL under #961434. We are extremely grateful to the TOPEX/Poseidon team at NASA/JPL and AVISO for providing the altimetry data. The Center for Ocean-Atmospheric Prediction Studies receives its base funding from ONR's Secretary of the Navy Grant, the NASA Physical Oceanography Program and through the Applied Research Center, funded by NOAA Office of Global Programs.

References

Le Dimet, F.X. and I. M. Navon, Variational and optimization methods in meteorology: a review. *Tech. Rep. FSU-SCRI-88-144*, Florida State University, Tallahassee, Florida, 83 pp., 1988.

Ghil, M. and P. Malonotte-Rizzoli, Data assimilation in meteorology and Oceanograpy, *Adv. Geophys.*, *33*, 141-266, 1991.

Kim, Kwang-Y., Statistical interpolation using cyclostationary EOFs, J. Clim., *11*, 2931-2942, 1997.

Morey, S. L., P. J. Martin, J. J. O'Brien, A. A. Wallcraft, and J. Zavala-Hidalgo, Export pathways for river discharged fresh water in the northern Gulf of Mexico, *J. Geophys. Res.*, *108*, 3303-3317, 2003.